Numerical simulation of internal tides and the resulting energetics within Monterey Bay and the surrounding area

S. M. Jachec,[1] O. B. Fringer,[1] M. G. Gerritsen,[1,2] and R. L. Street[1]

Received 15 March 2006; revised 10 May 2006; accepted 15 May 2006; published 24 June 2006.

[1] We use a three-dimensional nonhydrostatic unstructured-grid code to simulate internal tides within Monterey Bay. The predicted water surface, barotropic and baroclinic velocities, and internal tides in the greater coastal region agree with observations. The agreement is due to the use of a high-resolution mesh, alongshore prescription of the barotropic M_2 tidal velocities, and specification of initial conditions consistent with field data. Results of depth-integrated, M_2-period-averaged energy flux and energy flux divergence are presented in order to identify locations of significant internal wave generation and dissipation. Based on the results, there is a domain-wide power surplus of +52 MW due to internal tides that is available for pelagic mixing, yet isolated bathymetric features, such as Monterey Submarine Canyon and Smooth Ridge, are net dissipative, with dissipation rates of −8.3 and −1.5 MW, respectively.
Citation: Jachec, S. M., O. B. Fringer, M. G. Gerritsen, and R. L. Street (2006), Numerical simulation of internal tides and the resulting energetics within Monterey Bay and the surrounding area, *Geophys. Res. Lett.*, *33*, L12605, doi:10.1029/2006GL026314.

1. Motivation and Purpose

[2] *Toole et al.* [1994] suggest that average ocean mixing values may be dominated by coastal ocean processes. More recently, *Munk and Wunsch* [1998] advocated elevated mixing in the vicinity of rough coastal bathymetry due to tides. *Lien and Gregg* [2001], *Carter and Gregg* [2002], *Carter et al.* [2005], and *Gregg et al.* [2005] observe highly-concentrated intermittent patches of turbulence and diffusivity over ridges and within canyons. However, it is unclear how globally important local mixing process are to the energy budget [*Polzin et al.*, 1997; *Kunze et al.*, 2006]. Within the proximity of such bathymetric features, *Petruncio et al.* [1998] observe currents due to internal tides an order of magnitude larger than those in the surrounding area. This suggests that there may be a connection between enhanced mixing, elevated dissipation, and internal tides and internal waves in coastal ocean locations.

[3] Using numerical simulations with the Princeton Ocean Model (POM) [*Blumberg and Mellor*, 1987] and supplemented with field measurements, *Petruncio et al.* [2002] show using a simplified Monterey Bay domain that internal tides are generated at critical topography and observe that most of the energy propagates into the Monterey Submarine Canyon. Although their simulation results confirm the existence of a bottom-intensified current within the canyon, its magnitude is an order of magnitude lower than recorded in field measurements. In an attempt to improve their simulation, *Rosenfeld et al.* [1999] include realistic bathymetry with 1 km × 1 km grid spacing. However, this is found to be insufficient to raise simulated velocities to field magnitudes. To achieve results more consistent with field data, *Rosenfeld et al.* [1999] and *Petruncio et al.* [2002] suggest adding nonhydrostatic capabilities and including the alongshore component of the tidal velocity into the simulations.

[4] The purpose of this paper is to conduct three-dimensional simulations of the internal tides within Monterey Bay and the surrounding area. This is accomplished by applying the Stanford Unstructured Nonhydrostatic Terrain-following Adaptive Navier-Stokes Simulator (SUNTANS) [*Fringer et al.*, 2006] on a high-resolution grid and by remedying the shortcomings described by *Rosenfeld et al.* [1999] and *Petruncio et al.* [2002] to obtain the internal tidal velocity field. These results are used to compute internal tide energy flux and energy flux divergence to analyze internal tide energetics within Monterey Bay.

2. Simulation Technique

2.1. Physical Setting

[5] Monterey Bay (MB), California, is located 150 km south of San Francisco in northern California. Figure 1 shows the bathymetry of the bay and surrounding area. The region consists of the prominent east-west Monterey Submarine Canyon (MSC) flanked to the north and south by numerous smaller canyons, with a ridge located to the north of the canyon, and a continental slope and break region. Depths range from 0 to 3500 m with local steep gradients in bathymetry. While several locations within MB and the surrounding area are considered critical, locations where the beamlike internal tides may be generated, with respect to the M_2 tide, most of the baroclinic energy flux is in the low modes where tidal blocking arises [*Garrett and Kunze*, 2006] since energy within the higher modes is likely quickly lost to dissipation.

2.2. Description of the Numerical Method, Model Input, and Results

[6] SUNTANS is an unstructured, finite-volume, parallel coastal-ocean simulator that solves the incompressible three-dimensional nonhydrostatic Navier-Stokes equations with the Boussinesq approximation in a rotating frame along with equations for the free-surface, scalar transport of salinity and temperature, and equation of state for density.

[1]Environmental Fluid Mechanics Laboratory, Department of Civil and Environmental Engineering, Stanford University, Stanford, California, USA.
[2]Department of Petroleum Engineering, Stanford University, Stanford, California, USA.

0094-8276/06/2006GL026314$05.00

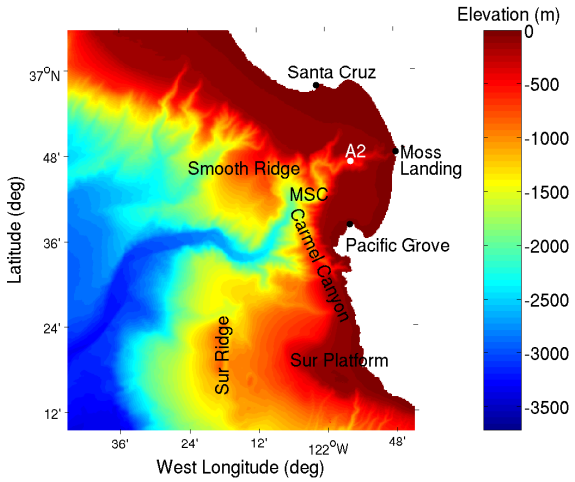

Figure 1. Bathymetry of Monterey Bay and surrounding area.

[7] A horizontal unstructured grid is generated for MB and the surrounding area. The domain extends from approximately 96 km south of Pacific Grove to Half Moon Bay in the north, and approximately 90 km offshore. The grid extent is similar to that of *Rosenfeld et al.* [2005], which allows adequate room for internal tides to be generated outside MB. The unstructured grid is composed of triangles and is built primarily along the depth contours. The coarsest grid resolution is about 1400 m along the offshore boundary while the resolution within Monterey Bay is approximately 290 m. The vertical resolution of the z-level grid is chosen to concentrate grid cells in the shallower regions, such as the shelf, yielding vertical grid spacing at the water surface of about 8 and 92 m in the deepest location. In total, the mesh consists of approximately three million cells, which provides adequate resolution to simulate internal tides. Once the grid is generated, bathymetric data, made available by the United States Geological Survey (USGS) and the Monterey Bay Aquarium Research Institute (MBARI), are interpolated onto the grid.

[8] At the coastline, we apply the no-flow condition, while the northern, southern, and offshore boundaries are considered open. For the open boundaries, an implementation of the clamped-free radiation condition [*Blumberg and Kantha*, 1985] is applied for the barotropic tide, while a radiation condition is used for the first-mode baroclinic velocity. The latter is purely radiated from the domain while the former allows the barotropic tidal component to be forced as well as radiated. Using the Oregon State University Tidal Solution for the U.S. West Coast [*Egbert et al.*, 1994], barotropic M_2 velocities (90% of the tidal signal) are prescribed uniformly in space and sinusoidally in time along the southern and northern boundaries with an amplitude of 5.0 cm s^{-1} and a time lag of five minutes between them, while the offshore boundary velocity varies sinusoidally with an amplitude of 0.4 cm s^{-1} and time lag of -22 minutes compared to the southern boundary. Although this results in a discontinuity at the open boundary corner, no observable effects are seen on the results. By using these amplitudes and phases, along with a timescale parameter of 48 minutes as part of the clamped-free radiation condition, M_2 water-surface heights consistent with field data are achieved. We do not prescribe baroclinic effects at the boundaries because we are primarily interested in where internal tides are generated and dissipated within the domain. Scalar boundary conditions are set as gradient-free while the simulation is initialized with scalar data consistent with work by *Rosenfeld et al.* [1994].

[9] The final inputs are numerical and physical parameters. A time step of 24 s satisfies the internal wave Courant condition while providing good temporal resolution. Since central differencing is used for advection of the momentum, a constant horizontal eddy viscosity of 20 m^2 s^{-1} is needed to keep the model stable. A vertical eddy viscosity of 2.0×10^{-3} m^2 s^{-1} is applied throughout the domain that is based on microstructure measurements recorded within the MSC [*Lueck and Osborn*, 1985] and the need to maintain numerical stability due to central differencing in the vertical direction. It is two orders of magnitude larger than the open ocean value. A bottom drag coefficient of 0.005, which is similar to one used by *Tseng* [2003] when modeling MB, and a Coriolis frequency of 8.7×10^{-5} rad s^{-1} are applied uniformly throughout the domain.

2.3. Validation of Simulation

[10] In this section we demonstrate that SUNTANS reproduces field results of velocity from the ITEX 1 experiment conducted in April 1994 [*Petruncio et al.*, 1998]. Since SUNTANS is forced using only the M_2 velocity component, it seems reasonable to make comparisons to the M_2 fit east-west velocities presented by *Petruncio et al.* [1998]. Figure 2 shows simulated east-west velocity (u) results from the nearest SUNTANS cells corresponding to Station A2. The color contours represent the velocity magnitude, and the black box represents the extent of the M_2-fit data from an ADCP located at Station A2. SUNTANS computes the currents well, including the location of the maximum current magnitude. In addition, it captures the semidiurnal flood-ebb pattern, and accurately simulates the vertical structure of the velocity, including downward phase propagation of the

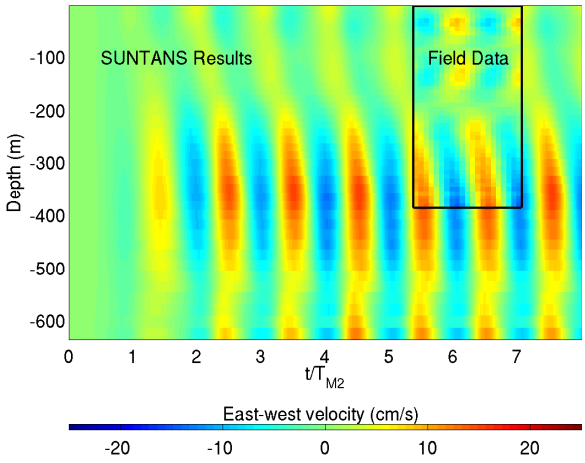

Figure 2. Simulation results from SUNTANS of East-West velocity with A2 field data overlaid.

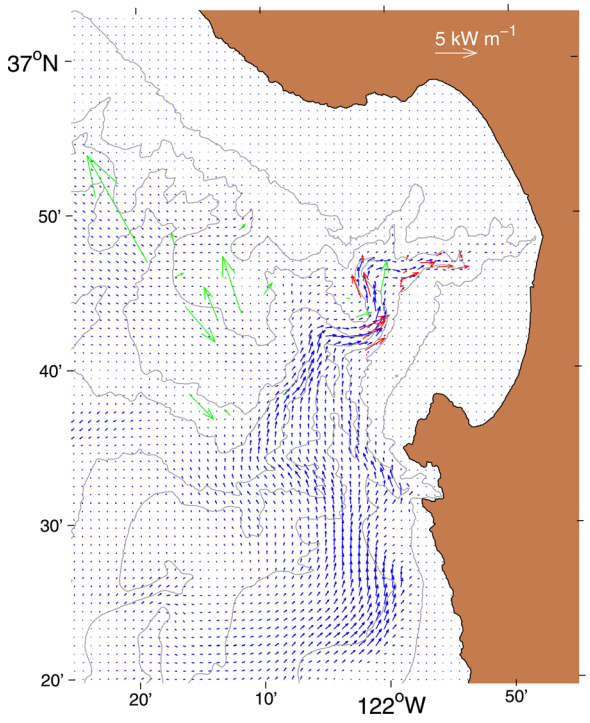

Figure 3. Depth-integrated, period-averaged baroclinic energy flux for Monterey Bay and surrounding area. Green field energy flux vectors have not been period averaged.

internal tide. Similar results are achieved for Station A1 and for other variables, such as the free surface and isopycnal displacements.

3. Understanding Internal Wave Energetics Via Energy Flux and Energy Flux Divergence

[11] The energy flux ($\mathbf{E_U}$) for baroclinic flows provides insight into the generation and the propagation of internal tides [*Cummins and Oey*, 1997]. We compute the depth-integrated ($\bar{}$), M_2-period-averaged ($\langle\ \rangle$) baroclinic energy flux for a water column as:

$$\langle \bar{\mathbf{E}}_\mathbf{U} \rangle = \frac{1}{T_{M_2}} \int_0^{T_{M_2}} \int_{-z}^{h} \vec{U}_{bc}\, p'\, dz'\, dt' \qquad (1)$$

where $\vec{U}_{bc}$ is the baroclinic velocity vector, p' is the fluctuating portion of the pressure, z is the local depth of interest, h is water surface of the column, and T_{M2} is the semidiurnal period, 12.42 hours.

[12] Figure 3 shows results of baroclinic energy flux (blue vectors). The majority of the energy flux is funneled into the MSC. The fluxes within the canyon seem to be steered by the canyon shape and decrease toward the canyon head, albeit non-monotonically. Within the canyon, results from SUNTANS yield energy flux vectors close to field fluxes (red vectors) from *Kunze et al.* [2002]. Outside the canyon, magnitudes and directions vary considerably between field data and simulated. However, *Kunze et al.* [2002] state that a set of their field energy fluxes represented as green vectors (primarily outside the canyon) are less reliable since they have not been averaged over a tidal cycle or may be contaminated by the California Undercurrent. Contrary to work by *Petruncio et al.* [1998] who identified Smooth Ridge and Sharp Ridge as possible generation sites of the internal tide energy entering into MSC, we find relatively little energy flux enters the canyon from these ridges, which is consistent with conclusions from *Kunze et al.* [2002].

[13] While the baroclinic energy flux provides insight to internal tide propagation, the baroclinic energy flux divergence ($\nabla \cdot \langle \bar{\mathbf{E}}_\mathbf{U} \rangle$) identifies generation sites (> 0 W m^{-2}) and dissipation sites (< 0 W m^{-2}) of internal tides [*Eich et al.*, 2004]. Internal tide generation locations tell us where barotropic energy is converted to baroclinic energy, while internal tide dissipation sites tell us where baroclinic energy is dissipated. Figure 4 shows the log-scale energy flux divergence in units of W m^{-2} for generation (left) and dissipation (right), respectively. Black contours represent

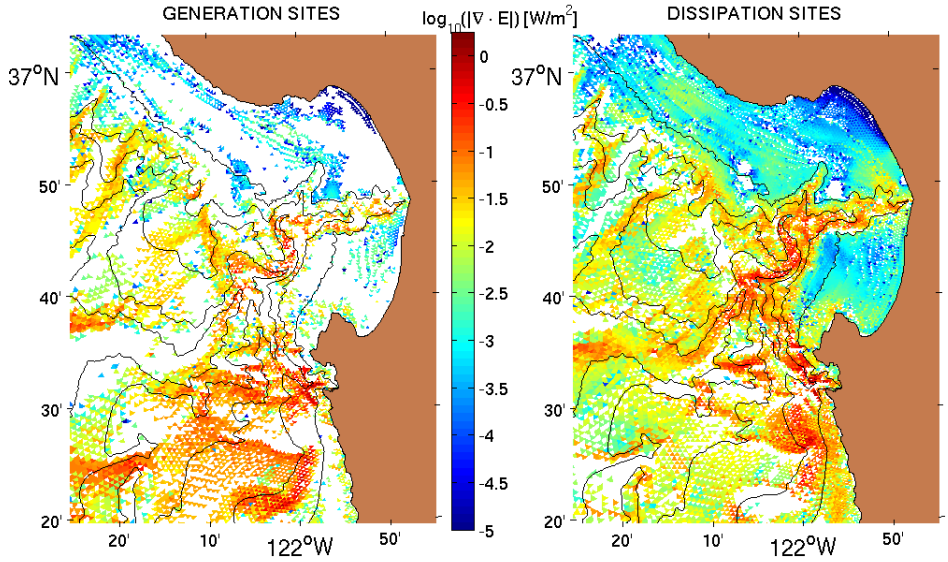

Figure 4. Depth-integrated, period-averaged baroclinic energy flux divergence for Monterey Bay and surrounding area.

the bathymetry. There are several key generation sites that are responsible for the majority of the simulated energy flux within the MSC. These locations are south of MB and include the Sur Platform and the surrounding area north of the Platform. While some local generation seems to be present within MSC, on the whole, there is net generation within the computational domain of +52 MW. Dissipation is widespread and locations of heightened dissipation occur in the vicinity of Sur Platform, within the MSC, and over the bulk of Smooth Ridge. Based on these numerical simulations, the latter locations have net dissipation of −8.3 and −1.5 MW, respectively. At present it is difficult to determine the mechanisms that are responsible for the dissipation. Possible physical mechanisms are bottom friction, wave breaking, and turbulence within hydraulic jumps. The former is currently being investigated by computing bottom shear stress due to baroclinic effects and will be reported in a future paper.

4. Summary and Conclusions

[14] Barotropic and baroclinic tides within Monterey Bay are simulated using SUNTANS, a three-dimensional, nonhydrostatic, unstructured, parallel code. The model is verified to reproduce water surface, isopycnal displacements, and velocities at several locations within the domain. A combination of high grid resolution (∼290 m within Monterey Bay) and alongshore barotropic tidal current boundary conditions lead to improved velocity and isopycnal results. Energetics for Monterey Bay are computed using the energy flux and the energy flux divergence in order to identify baroclinic energy sources that represent internal tide generation, and baroclinic energy sinks that represent dissipation. Energy flux and energy flux divergence show that Sur Platform and a region north of the Sur Platform are responsible for a majority of the numerically observed baroclinic energy flux within the MSC, while local generation within the MSC is isolated. Based on the entire computational domain there is +52 MW available for pelagic mixing supporting the ideas of *Munk and Wunsch* [1998] and *Lien and Gregg* [2001]. The dissipation of internal tides is widespread, but notable dissipation sites are the Sur Platform region, MSC (−8.3 MW), and Smooth Ridge (−1.5 MW). Next steps will include investigating the sea floor and mid-water column generation and dissipation of internal tidal energy by assessing the vertical distribution of energy and energy flux.

[15] **Acknowledgments.** The authors gratefully acknowledge the support of ONR grant N00014-05-1-0294 (Scientific officers: C. Linwood Vincent, Terri Paluszkiewicz, and Scott Harper). Simulations were carried out on the JVN cluster at the ARL Major Shared Resource Center and the Baywulf cluster at the Peter A. McCuen Environmental Computing Center at Stanford University. We would also like to thank Emil Petruncio from the United States Naval Academy and Leslie Rosenfeld and Jeff Paduan from the Naval Postgraduate School for their help in obtaining and using field data from the ITEX1 experiments. Bathymetry data is provided by USGS and MBARI. We also thank Eric Kunze, Mike Gregg, and Glenn Carter for supplying us with energy flux data. Comments from two anonymous reviewers greatly improved the manuscript.

References

Blumberg, A. F., and L. H. Kantha (1985), Open boundary conditions for circulation models, *J. Hydrol. Eng.*, *11*, 237–255.

Blumberg, A. F., and G. L. Mellor (1987), A description of a three-dimensional coastal ocean circulation model, in *Three-Dimensional Coastal Ocean Models*, *Coastal Estuarine Ser.*, vol. 4, edited by N. S. Heaps, pp. 1–16, AGU, Washington, D. C.

Carter, G. S., and M. C. Gregg (2002), Intense, variable mixing near the head of Monterey Submarine Canyon, *J. Phys. Oceanogr.*, *32*, 3145–3165.

Carter, G. S., M. C. Gregg, and R.-C. Lien (2005), Internal waves, solitary-like waves, and mixing on the Monterey Bay shelf, *Cont. Shelf Res.*, *25*, 1499–1520.

Cummins, P. F., and L. Oey (1997), Simulation of barotropic and baroclinic tides off northern British Columbia, *J. Phys. Oceanogr.*, *27*, 762–781.

Egbert, G. D., A. F. Bennett, and M. G. G. Foreman (1994), TOPEX/POSEIDON tides estimated using a global inverse model, *J. Geophys. Res.*, *99*(C12), 24,821–24,852.

Eich, M. L., M. A. Merrifield, and M. H. Alford (2004), Structure and variability of semidiurnal internal tides in Mamala Bay, Hawaii, *J. Geophys. Res.*, *109*, C05010, doi:10.1029/2003JC002049.

Fringer, O. B., M. G. Gerritsen, and R. L. Street (2006), An unstructured-grid, finite-volume, nonhydrostatic, parallel coastal ocean simulator, *Ocean Modell.*, in press.

Garrett, C., and E. Kunze (2006), Internal tide generation in the deep ocean, *Annu. Rev. Fluid Mech.*, in press.

Gregg, M. C., G. S. Carter, and E. Kunze (2005), Corrigendum, *J. Phys. Oceanogr.*, *35*, 1712–1715.

Kunze, E., L. K. Rosenfeld, G. Carter, and M. C. Gregg (2002), Internal waves in Monterey Submarine Canyon, *J. Phys. Oceanogr.*, *32*, 1890–1913.

Kunze, E., E. Firing, J. Hummon, T. Chereskin, and A. Thurnherr (2006), Global abyssal mixing inferred from lowered ADCP shear and CTD strain profiles, *J. Phys. Oceanogr.*, in press.

Lien, R.-C., and M. Gregg (2001), Observations of turbulence in a tidal beam and across a coastal ridge, *J. Geophys. Res.*, *106*(C3), 4575–4591.

Lueck, R. G., and T. R. Osborn (1985), Turbulence measurements in a submarine canyon, *Cont. Shelf Res.*, *4*, 1831–1833.

Munk, W., and C. Wunsch (1998), Abyssal recipes II: Energetics of tidal and wind mixing, *Deep Sea Res., Part I*, *45*, 1977–2010.

Petruncio, E. T., L. K. Rosenfeld, and J. D. Paduan (1998), Observations of the internal tide in Monterey Canyon, *J. Phys. Oceanogr.*, *28*, 1873–1903.

Petruncio, E. T., J. D. Paduan, and L. K. Rosenfeld (2002), Numerical simulation of the internal tide in a submarine canyon, *Ocean Modell.*, *4*, 221–248.

Polzin, K. L., J. M. Toole, J. R. Ledwell, and R. W. Schmitt (1997), Spatial variability of turbulent mixing in the abyssal ocean, *Science*, *276*, 306–328.

Rosenfeld, L. K., R. E. Schramm, J. B. Hatcher, and T. Anderson (1994), Hydrographic data collected in Monterey Bay during 1 September 1988 to 16 December 1992, *Tech. Rep. 94-15*, Monterey Bay Aquarium Res. Inst., Monterey, Calif.

Rosenfeld, L. K., J. D. Paduan, E. T. Petruncio, and J. E. Gonclaves (1999), Numerical simulations and observations of the internal tide in a submarine canyon, paper presented at 11th 'Aha Huliko'a Hawaiian Workshop: Dynamics of Oceanic Internal Gravity Waves, Univ. of Hawaii at Manoa, Honolulu, Hawaii.

Rosenfeld, L. K., I. Shulman, M. Cook, and L. S. J. Paduan (2005), Development of a tidal model for central California, paper presented at Sixth Conference on Coastal Atmospheric and Oceanic Prediction and Processes, Am. Meteorol. Soc., San Diego, Calif.

Toole, J. M., K. L. Polzin, and R. W. Scmitt (1994), Estimates of diapycnal mixing in the abyssal ocean, *Science*, *264*, 1120–1123.

Tseng, Y.-H. (2003), On the development of a ghost-cell immersed boundary method and its application to large eddy simulation and geophysical fluid dynamics, Ph.D. thesis, Stanford Univ., Stanford, Calif.

O. B. Fringer, M. G. Gerritsen, S. M. Jachec, and R. L. Street, Environmental Fluid Mechanics Laboratory, Department of Civil and Environmental Engineering, Stanford University, Stanford, CA 94305, USA. (sjachec@stanford.edu)